AIMS Energy, 7(5): 671–687.
DOI: 10.3934/energy.2019.5.671
Received: 01 September 2019
Accepted: 23 October 2019
Published: 25 October 2019

http://www.aimspress.com/journal/energy

Research article

Recognition of disturbances in hybrid power system interfaced with battery energy storage system using combined features of Stockwell transform and Hilbert transform

Virendra Sharma* and Lata Gidwani

Department of Electrical Engineering, Rajasthan Technical University, Kota, India

*** Correspondence:** Email: vsharmakiran@gmail.com.

Abstract: This paper presents an algorithm using combined features of Stockwell transform and Hilbert transform for analysis of disturbances in the hybrid power system interfaced with battery energy storage system (BESS). Hybrid power system is realized using five nodes test network to which BESS supported by distribution static compensator (DSTATCOM), wind and solar photovoltaic (PV) generators are integrated. A disturbance detection index (DDI) based on combined features of Stockwell transform and Hilbert transform is proposed for detection of various types of disturbances. Results are obtained in the absence and presence of the proposed BESS supported by DSTATCOM to investigate the effect of BESS on performance of the hybrid power system. Investigated events include the switching ON/OFF the resistive load, outage of wind generator and simultaneous outage of both wind and solar PV generators. It is anticipated that performance of proposed method will be high in all investigated cases of study. This could be established in MATLAB/Simulink environment. Proposed BESS will be effective to reduce the disturbance level up to 91%.

Keywords: battery energy storage system; distribution static compensator; Hilbert transforms; hybrid power system; Stockwell transform

1. Introduction

Renewable energy (RE) sources such as wind energy and solar photovoltaic (PV) energy systems have been integrated to the existing utility grid in recent years to form hybrid power system

network to meet out future energy demand. This has leads to problems related to stability, protection and power quality (PQ). The RE sources may affect both the voltage and current quality in the hybrid system. The proper diagnosis of disturbances is required to initiate a mitigation approach [1]. The custom power devices such as dynamic voltage restorer (DVR), static VAR compensator (SVC), distribution static compensator (DSTATCOM) and unified power flow controller may be implemented to improve the quality of power with renewable energy penetration in the utility grid by reducing the level of disturbances [2]. In [3], authors presented a non-linear controller design for a DSTATCOM which is connected to a distribution network integrated with distributed generator (DG) used to regulate the line voltage by providing reactive power compensation. A method to produce maximum power from a solar PV system, a hybrid method using fuzzy-neural is proposed in [4,5]. Authors implemented various case studies to establish effectiveness and superiority of the proposition by achieving good dynamic operation, faster convergence speed, less oscillations of operating point around maximum power point (MPP). An improved version of control method based on Fuzzy Gain Scheduling of Proportional-Integral-Derivative (FGS-PID) controller has been proposed for a hybrid Photovoltaic (PV) and Battery Energy Storage (BES) system under different weather conditions in [6]. Proposed controller is implemented with the help of a two-level control system resulting in advantages of the PID as well as the fuzzy logic controller (FLC) for tracking maximum power point. A hybrid robust-stochastic method considering the load uncertainty, temperature and wind speed, the amount of solar radiation and the cost of purchasing energy suitable for bidding of hybrid energy sources including wind micro turbines, energy storage systems, renewable energy sources (wind turbine and solar system) and bilateral contracts is proposed in [7]. A new topology for a hybrid generation system incorporated with PV and wind turbine using a hybrid fuzzy-neural maximum power point tracking (MPPT) method to capture the maximum power is reported in [8].

Digital signal processing techniques like Fourier transform (FT), short-time Fourier transform (STFT), wavelet transform (WT), Kalman filter, and Stockwell transform (ST) are effective in detection of operational events. These methods use the time and frequency domain information to achieve detection of operational events. The FT does perform with low efficiency for detection of islanding events. STFT decomposes the non-stationary signal into time-frequency domain by considering it as a concatenation of stationary signals within the sliding window. Wavelet analysis allows the use of long time intervals for precise low frequency information and shorter regions for high frequency information. The ST combines the elements of WT and STFT but falls in different category. It uses an analysis window whose width is decreasing with the frequency, providing a frequency-dependent resolution [9]. The detection of islanding events and operational events include the feature extraction of a disturbance from the current and voltage signals. The signal processing techniques such as Fourier Transform (FT), short time Fourier Transform (STFT), wavelet transform (WT), Stockwell's Transform (S-transform), Gabor Transform etc. have been utilized for the feature extraction to detect the islanding and operational events [10]. In [11], authors presented a new time-frequency algorithm for detection of power islanding event in distributed generation based hybrid power system using a hybrid fast variant of the S-Transform (ST) algorithm and a fuzzy expert system. It is pointed out that, very less number of articles is available on the detection of disturbances in the utility grid with renewable energy penetration using the combined features of signal processing technique. Hence, there is a need to investigate the alternative methods based on combined features of signal processing techniques to detect disturbances in the utility network. A new method for Combined Heat and Power (CHP)

unit islanding detection using Kriging Empirical Mode Decomposition (KEMD) and Support Vector Machine (SVM) pattern learning algorithm is reported in [12]. In proposed algorithm the variation of Intrinsic Mode Functions (IMF) of local signals in two-dimensional mode is used as relay input data. An optimal signal selection model is proposed for relay for Non-Detection Zone (NDZ). In [13], thermal conducting behaviour of carbon nanotube (CNT)-reinforced metal matrix nano-composites (MMNCs) has been studied using a micromechanical model based on the method of cell (MOC) algorithm. A new algorithm for detection of islanding events in a hybrid power system having distributed generation (DG) sources using Hilbert–Huang transform (HHT) and Extreme learning machine (ELM) is presented in [14].

This paper proposed a battery energy storage system controlled by DSTATCOM to reduce the level of disturbances in the utility network. Further, a technique based on the combined features of Stockwell transform and Hilbert transform is proposed for detection of the disturbances in the utility grid. The disturbances are detected with and without the BESS to show the effectiveness of proposed BESS in reducing the disturbance level.

This paper is organized in to five sections. Introduction is presented in Section 1. Section 2 describes the test system and proposed BESS supported by distribution static compensator. Proposed algorithm is presented in Section 3. Simulation results and their discussions are presented in Section 4. Conclusions are included in Section 5.

2. Test system

Test network of hybrid power system (HPS) used for study related to detection of disturbances with and without battery energy storage system is detailed in this section. Details of wind energy conversion system (WECS), solar photovoltaic (PV) system and BESS supported by DSTATCOM used in the study are also provided in this section.

2.1. Test network

Test network of HPS integrated to Utility grid and interfaced with doubly fed induction generator (DFIG) based wind energy generation system, solar PV system and BESS is described in Figure 1. Generator G1 used to represent utility grid is integrated through a generator transformer (XFM) to bus B2. Transmission lines of the test network are represented by TRL1, TRL2 and TRL3. Transmission line parameters are detailed in Table 1. All loads have values equal to 2 MW. Details of transformers used in the test network are provided in Table 2.

Table 1. Transmission line parameters of test system.

S. No.	Transmission Line Parameters	values
1	Positive sequence impedance	0.1153 + j0.3958 Ω/km
2	Zero sequence impedance	0.4130 + j1.2516 Ω/km
3	Length of transmission line TRL1	14 km
4	Length of transmission line TRL2	14 km
5	Length of transmission line TRL3	2.5 km

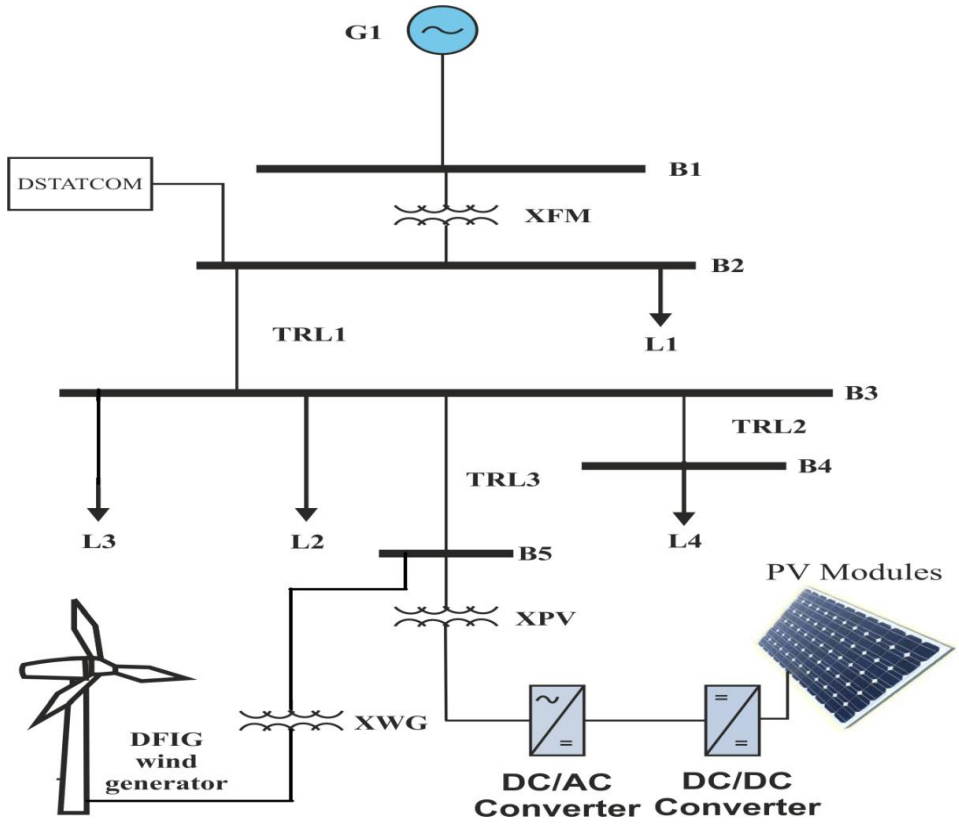

Figure 1. Hybrid power system.

Table 2. Transformer parameters of test system.

Transformer symbol	MVA Rating	Voltage HV winding (kV)	Voltage LV winding (kV)
XFM	47	120	4.16
XPV	1	4.16	0.260
XWG	3	4.16	0.575

2.2. Wind energy conversion system

Wind energy conversion system (WECS) used for the proposed study is consists of the components such as wind turbine (WT), rotor side converter (RSC), grid side converter (GSC), a doubly fed induction generator (DFIG) and a dc link capacitor. Wind turbine is used to convert kinetic energy of wind speed into mechanical energy of shaft. This mechanical energy is converted to electrical energy using DFIG. WECS used in the study has a rating of 1.5 MW and 60 Hz frequency. The power is delivered at voltage level of 575 V. WECS is integrated to utility grid through transformer XWG. The wind speed equal to 11 m/s is used in this study. Parameters reported in [15] are considered for modeling of WECS. The generator data (for each generator) are as follows: H (inertia constant) = 0.685 s, *Rs* = 0.023 *pu*, *Ls* = 0.18 *pu*, *Rr* = 0.016 *pu*, *Lr* = 0.016 *pu*, *Lm* = 2.9 *pu*. Maximum pitch angle is 27 ° and maximum rate of change of pitch angle is 10 °/s. Pitch controller gain is 150. Reactive power and voltage regulator gains are 0.05 and 20 respectively.

2.3. Solar PV system

The solar PV system rated at 100 kW is integrated to test network on bus B5 using a transformer designated as XPV. Technical parameters of the solar PV system as reported in [16] are used in the proposed study. The solar PV array consists of 66 parallel strings and each string has 5 modules connected in series. At standard test conditions (STC), each module has *Voc* = 64.2 *V*, *Isc* = 5.96 *A*, *Vmp* = 54.7 *V*, *Imp* = 5.58 *A*, *Rs* = 0.037998 Ω, *Rp* = 993.51 Ω, *Isat* = 1.1753 *e*−8 *A*, *Iph* = 5.9602 *A*. Output direct current (dc) voltage of solar PV system is 273.5 V which is stepped up to 500 V dc using a dc-dc boost converter. A dc to ac inverter is used to convert 500 V dc into 260 V three phase ac Supply. This is stepped up to 4.16 kV using transformer XPV.

2.4. Battery energy storage system

Battery energy storage system is integrated on bus B2 of hybrid test power system using three-leg topology of three-phase three-wire DSTATCOM. BESS is connected in parallel with the DC link capacitor of DSTATCOM as shown in Figure 2. Active and reactive powers can be exchanged between the DSTATCOM supported BESS and HPS network by varying voltage magnitude of the inverter and phase angle difference between bus voltage and the inverter output [17]. Active and reactive powers exchange can be given by following relations:

$$P = \frac{V_{pcc} V_c \sin(\alpha)}{X} \tag{1}$$

$$Q = \frac{V_{pcc}(V_{pcc} - V_c \cos(\alpha))}{X} \tag{2}$$

where V_c is the inverter voltage; P is the active power exchange; Q is the reactive power exchange; V_{pcc} is the voltage at point of common coupling (PCC); α is the angle of V_{pcc} with respect to V_c; X is the reactance of the coupling inductor.

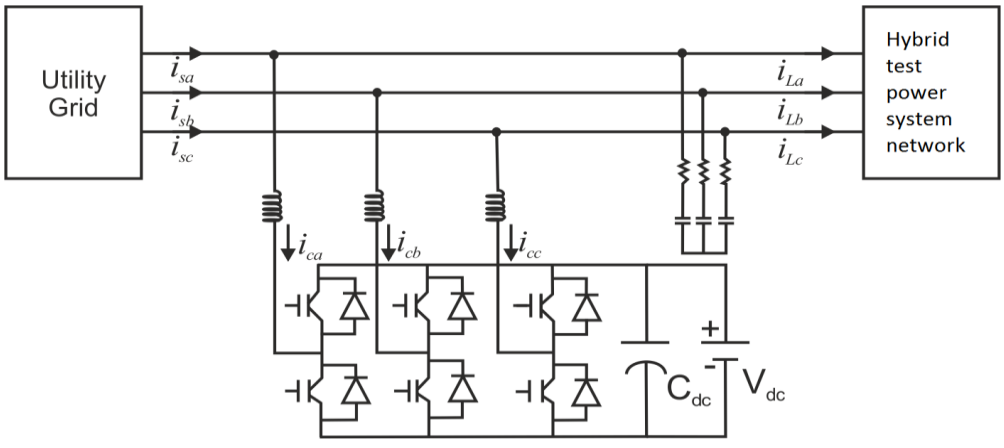

Figure 2. Battery energy storage system integrated to hybrid power system using DSTATCOM.

The design value of the dc link capacitor used in this study is 10,000 μF which is calculated

using the relations reported in [18]. The design value of ac inductor is selected as 40 mH using the relations reported in [19]. The resistance and inductance of the ripple filter are taken as 0.1 Ω and 10 μF respectively based on the constraints reported in [20]. Voltage of the battery energy storage system is kept at 7000 V and calculated using the relations reported in [21].

3. Algorithm proposed for disturbance detection

A brief description of the Stockwell transform, Hilbert transform and proposed algorithm are detailed in the following subsections.

3.1. Stockwell transform

The Stockwell Transform (ST) had been introduced first time by R. G. Stockwell. It is the elaborated form of continuous WT (CWT). Message to be communicated is contained in phase and amplitude of Stockwell transform. Mother wavelet is essential that phase may be changed so that information in CWT phase will be effective. Discrete ST may be easily evaluated by using good efficiency of Fast Fourier Transform (FFT) and convolution theorem. Result of Stockwell transform is extracted in the form of a matrix known as S-matrix which is complex in nature. Each row of the matrix indicates a certain frequency and every column show definite time. S-matrix elements are complex values by nature. ST-amplitude (STA) matrix is extracted by taking absolute values of S-matrix elements. Hence, high time resolution is achieved with a high frequency and a low time resolution at a low frequency. S-Transform uses multi-resolution with window width which changes inversely proportional to frequency. Power data are changing with respect to time. Hence, high time resolution at high frequency and low time resolution at low frequency are maintained. It is introduced that a relationship between STFT and *S*-transform and type of deriving *S*-transform from "phase correction" of CWT. Short time Fourier Transform of a signal h(t) is defined by following relation.

$$STFT(\tau, f) = \int_{-\infty}^{+\infty} h(t) g(\tau - t) e^{-j2\pi f t} dt \tag{3}$$

where τ and f indicate respectively time of spectral location and Fourier frequency where $g(t)$ indicate a window function. S-transform may be derived from above equation by replacement of window function $g(t)$ with Gaussian function as detailed below.

$$g(t) = \frac{|f|}{\sqrt{2\pi}} e^{-\frac{f^2 t^2}{2}} \tag{4}$$

Then S-transform is described as below.

$$S(\tau, f) = \int_{-\infty}^{+\infty} h(t) \frac{|f|}{\sqrt{2\pi}} e^{\frac{f^2(\tau - t)^2}{2}} e^{-j2\pi f t} dt \tag{5}$$

Hence, S-transform derived from STFT with Gaussian window function. If window of S-transform is wider in time domain, S-transform can provide better frequency resolution for lower frequency. While window is narrower, it can provide better time resolution for higher frequency. Output of

S-transform is a matrix called S-matrix. Information pertaining to frequency and amplitude of signal may be extracted from S-matrix.

3.2. Hilbert transform

The purpose of Hilbert transform (HT) is used as a spectral analysis tools for providing the time-frequency-energy description of time series data. Also, these methods describe non-stationary data locally. The Hilbert transform was used, in order to compute instantaneous frequencies and amplitudes and describe the signal more locally. Hilbert transform can be written for any function x(t) by the following relation where PV denotes Cauchy's principle value integral.

$$H[x(t)] = \frac{1}{\pi} PV \int_{-\infty}^{\infty} \frac{x(\tau)}{t-\tau} d\tau \tag{6}$$

3.3. Proposed algorithm

Proposed algorithm used for the detection of disturbances in the hybrid power system network can be implemented with following steps.

- The various case studies are simulated with the help of test system described in the section 2. The current signals are recorded at the PCC which is point of interfacing of the proposed test system with the utility grid.
- Current signals are decomposed using mathematical relations of Stockwell Transform presented in section 3.1 to obtain the output S-matrix in MATLAB software.
- A median of S-matrix is obtained and designated as ST-index. This plot is plotted with respect to time.
- The current signals are decomposed using mathematical relation of the Hilbert Transform provided in section 3.2 in MATLAB software and absolute values of output is obtained and designated as H-index.
- Multiplication of ST-index and H-index is obtained by multiplying element by element and resultant index is designated as disturbance detection index (DDI). The relative peak of DDI helps to detect the level of disturbances in the utility network of hybrid power system.

4. Simulation results and discussion

This section details the simulation results related to various case studies such as switching ON the resistive load, switching OFF the resistive load, outage of wind generator and outage of both wind and solar PV generators with and without BESS. However, event of outage of solar PV system is similar to the outage of wind plant alone; hence due to page limitation results of outage of solar PV alone are not included. Discussion of simulation results is also provided in this section.

4.1. Switching on the resistive load

An additional resistive load (other than L1, L2, L3 and L4) rated at 2 MW is switched on at 0.5 s without BESS. Current signal is recorded at PCC and depicted in Figure 3(a). Current corresponding

to phase-A is decomposed using Stockwell transform and median of absolute values of the output S-matrix is obtained and designated as ST-index which is illustrated in Figure 3(b). This current signal is also decomposed using the Hilbert transform and absolute values of the output is designated as H-index as illustrated in Figure 3(c). Element by element multiplication of proposed ST-index and H-index is obtained and designated as DDI as illustrated in Figure 3(d).

This can be observed from the Figure 3(b) that at the time of switching on the resistive load, the ST-index takes high value. However, this index has zero values before the event of switching on the resistive load indicating that significant disturbances are introduced in the current signal. Further, after the occurrence of event low magnitude transients are also observed. This is observed from the Figure 3(c) that at the time of switching on the resistive load, values of H-index increase from 650 to 1000 indicating that current drawn from the source has increased. A small magnitude transient peak observed at the time of event occurrence indicates that disturbances are introduced in the current signal. This can be observed from the Figure 3(d) that at the time of switching on the resistive load, the proposed DDI takes high values indicating that significant disturbances are introduced in the current signal. However, this index has zero values before the event of switching on the resistive load. Further, after the event of switching on the resistive load significant transient components have been observed. This index takes care of the disturbances introduced due to both magnitude and frequency transient components.

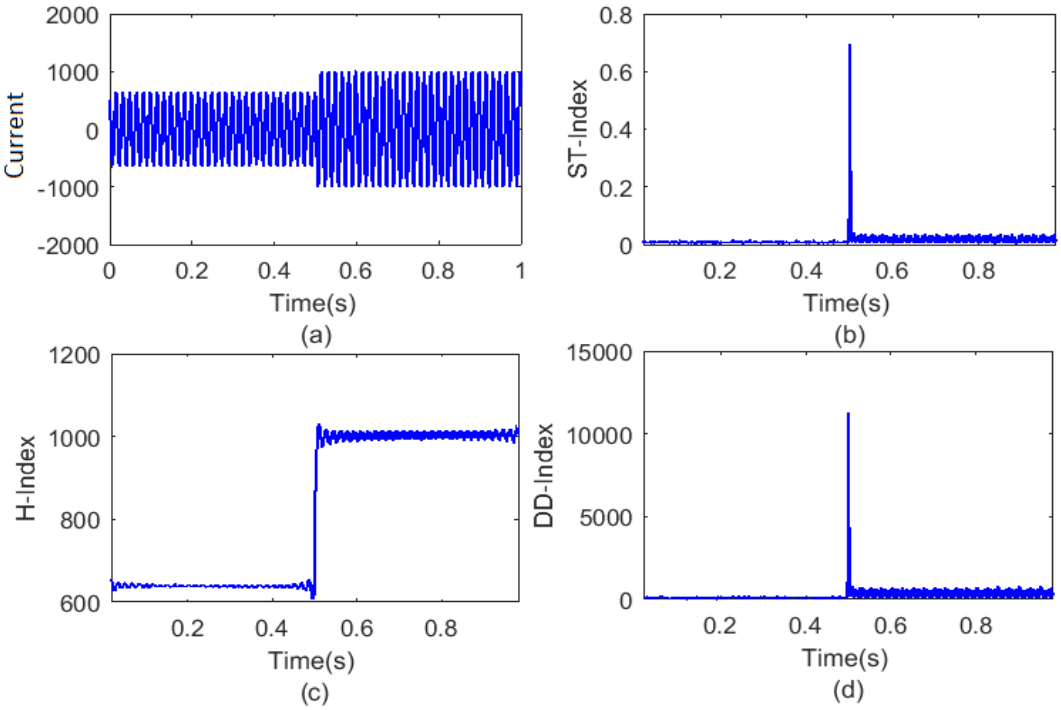

Figure 3. Event of switching on the resistive load without BESS (a) current signal (b) ST-index (c) H-index (d) disturbance detection index.

A resistive load rated at 2 MW is switched on at 0.5 s in the presence of battery energy storage system. Current signal is recorded at PCC and depicted in Figure 4(a). Current corresponding to phase-A is decomposed using Stockwell transform and median of absolute values of the output

S-matrix is obtained and designated as ST-index which is illustrated in Figure 4(b). This current signal is also decomposed using the Hilbert transform and absolute values of the output is designated as H-index as illustrated in Figure 4(c). Element by element multiplication of proposed ST-index and H-index is obtained and designated as DDI as illustrated in Figure 4(d).

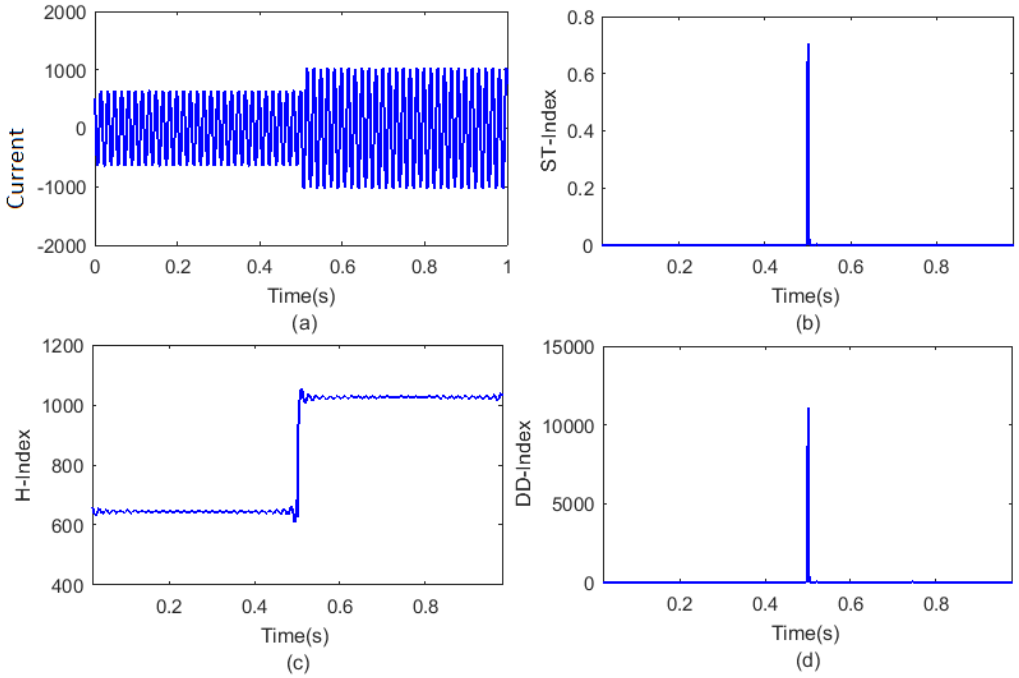

Figure 4. Event of switching on the resistive load with BESS (a) current signal (b) ST-index (c) H-index (d) disturbance detection index.

This can be observed from the Figure 4(b) that at the time of switching on the resistive load, the ST-index takes high values. However, this index has zero values before the event of switching on the resistive load. Further, the low magnitude transients are observed after the event has been eliminated by the use of BESS. This is observed from the Figure 4(c) that at the time of switching on the resistive load, values of H-index increase from 650 to 1050 indicating that current drawn from the source has been increased. Hence, by the use of BESS improvement in the current magnitude has been observed. A small magnitude transient peak observed at the time of event occurrence indicates that disturbances are introduced in the current signal. This can be observed from the Figure 4(d) that at the time of switching on the resistive load, the proposed DDI takes high values indicating that significant disturbances are introduced in the current signal. However, this index has zero values before the event of switching on the resistive load. Disturbance level has been reduced by 10% during the event of switching on the resistive load in the presence of BESS. Further, after the event of switching on the resistive load the transient components have been eliminated completely by the use of BESS.

4.2. Switching off the resistive load

A resistive load rated at 2 MW already connected on bus B2 of test system is switched OFF at 0.5 s

in the absence of BESS. Current signal is recorded at PCC and depicted in Figure 5(a). Current corresponding to phase-A is decomposed using Stockwell transform and median of absolute values of the output S-matrix is obtained and designated as ST-index which is illustrated in Figure 5(b). This current signal is also decomposed using the Hilbert transform and absolute values of the output is designated as H-index and illustrated in Figure 5(c). Element by element multiplication of proposed ST-index and H-index is obtained and designated as DDI and illustrated in Figure 5(d).

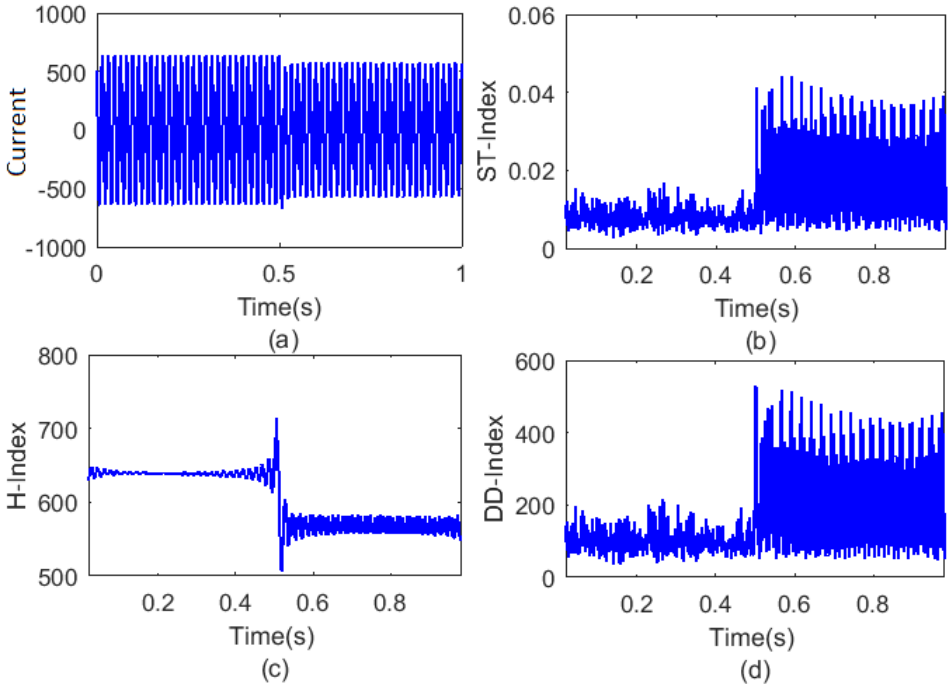

Figure 5. Event of switching off the resistive load without BESS (a) current signal (b) ST-index (c) H-index (d) disturbance detection index.

This can be observed from the Figure 5(b) that at the time of switching OFF the resistive load, the ST-index takes high values. However, this index has low values before the event of switching OFF the resistive load indicating that significant disturbances are introduced in the current signal. Further, after the occurrence of event, high magnitude transients are also observed. This is observed from the Figure 5(c) that at the time of switching OFF the resistive load, values of H-index decrease from 650 to 550 indicating that current drawn from the source has decreased. A small magnitude transient peak observed at the time of event occurrence indicates that disturbances are introduced in the current signal. This can be observed from the Figure 5(d) that at the time of switching OFF the resistive load, the proposed DDI takes high values indicating that significant disturbances are introduced in the current signal. However, this index has low values before the event of switching OFF the resistive load. Further, after the event of switching OFF the resistive load significant transient components of high magnitude have been observed.

A resistive load rated at 2 MW already connected on bus B2 of the test system is switched OFF at 0.5 s in the presence of BESS. Current signal is recorded at PCC and depicted in Figure 6(a). Current corresponding to phase-A is decomposed using Stockwell transform and median of absolute

values of the output S-matrix is obtained and designated as ST-index which is illustrated in Figure 6(b). This current signal is also decomposed using the Hilbert transform and absolute values of the output is designated as H-index and illustrated in Figure 6(c). Element by element multiplication of proposed ST-index and H-index is obtained and designated as DDI and illustrated in Figure 6(d).

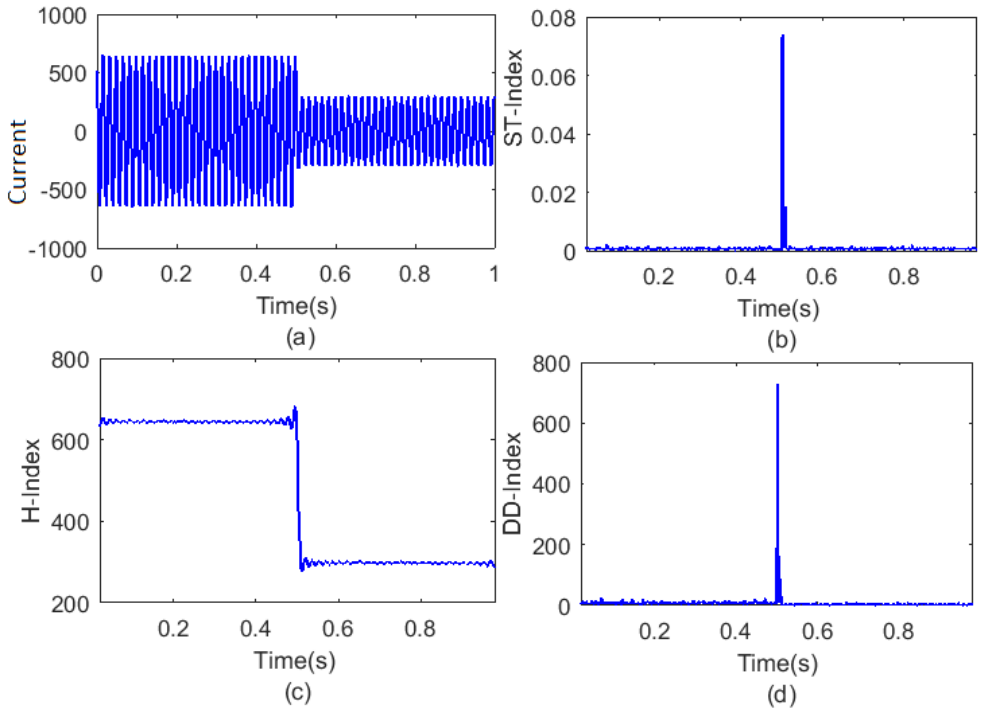

Figure 6. Event of switching off the resistive load with BESS (a) current signal (b) ST-index (c) H-index (d) disturbance detection index.

This can be observed from the Figure 6(b) that at the time of switching OFF the resistive load in the presence of BESS, the ST-index takes high values. However, this index has zero values before the event of switching OFF the resistive load. Further, the transients after the event have been eliminated by the use of BESS. This is observed from the Figure 6(c) that at the time of switching OFF the resistive load, values of H-index decrease from 650 to 300 indicating that current drawn from the source has been decreased and BESS has supplied a part of the load. Hence, by the use of BESS improvement in the current magnitude has been observed. A small magnitude transient peak observed at the time of event occurrence indicates that disturbances are introduced in the current signal and significant improvement has been observed by the use of BESS. This can be observed from the Figure 6(d) that at the time of switching OFF the resistive load, the DDI takes high values indicating that significant disturbances are introduced in the current signal. This is due to power electronic converter of the DSTATCOM. However, this index has zero values before the event of switching on the resistive load. Further, after the event of switching on the resistive load the transient components have been eliminated completely by the use of BESS.

4.3. Outage of wind generator

Wind generator integrated on bus B5 of test system is switched OFF at 0.5 s in the absence of BESS. Current signal is recorded at PCC and depicted in Figure 7(a). Current corresponding to phase-A is decomposed using Stockwell transform and median of absolute values of the output S-matrix is obtained and designated as ST-index which is illustrated in Figure 7(b). This current signal is also decomposed using the Hilbert transform and absolute values of the output is designated as H-index as illustrated in Figure 7(c). Element by element multiplication of proposed ST-index and H-index is obtained and designated as DDI as illustrated in Figure 7(d).

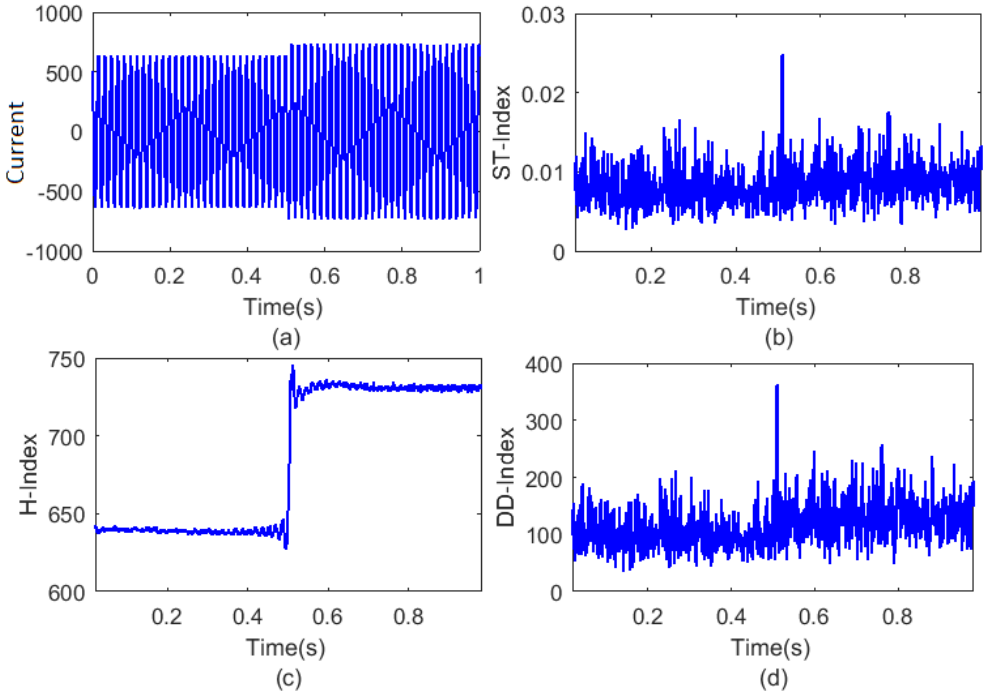

Figure 7. Event of outage of wind generator without BESS (a) current signal (b) ST-index (c) H-index (d) disturbance detection index.

This can be observed from the Figure 7(b) that at the time of outage of wind generator, the ST-index takes high value. However, this index has low values before the event of outage of wind generator indicating that significant disturbances are introduced in the current signal. Further, after the occurrence of event the transients with significant magnitude are also observed. This is observed from the Figure 7(c) that at the time of outage of wind generator, values of H-index increase from 640 to 740 indicating that current drawn from the source has increased. A small magnitude transient peak observed at the time of event occurrence indicates that disturbances are introduced in the current signal. This can be observed from the Figure 7(d) that at the time of outage of wind generator, the proposed DDI takes high values of 350 indicating that significant disturbances are introduced in the current signal. However, this index has values with significant magnitude before the event of outage of wind generator. Further, after the event of outage of wind generator transient components of significant magnitude are also observed.

Wind generator integrated on bus B5 of test system is switched OFF at 0.5 s in the presence of BESS. Current signal is recorded at PCC and depicted in Figure 8(a). Current corresponding to phase-A is decomposed using Stockwell transform and median of absolute values of the output S-matrix is obtained and designated as ST-index which is illustrated in Figure 8(b). This current signal is also decomposed using the Hilbert transform and absolute values of the output is designated as H-index as illustrated in Figure 8(c). Element by element multiplication of proposed ST-index and H-index is obtained and designated as DDI as illustrated in Figure 8(d).

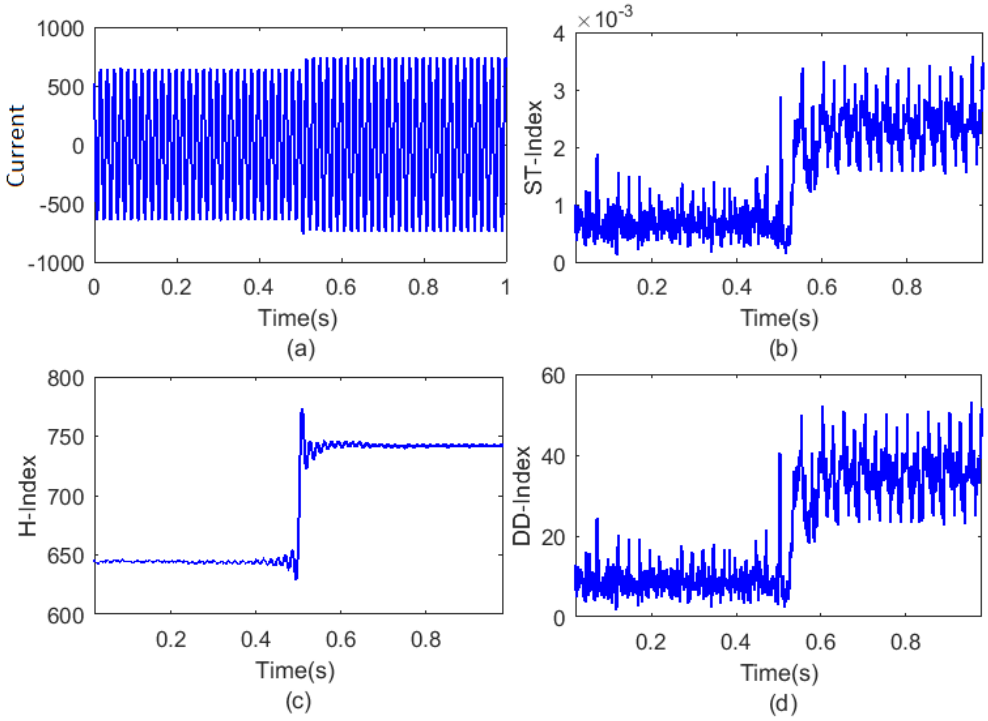

Figure 8. Event of outage of wind generator with BESS (a) current signal (b) ST-index (c) H-index (d) disturbance detection index.

This can be observed from the Figure 8(b) that at the time of outage of wind generator in the presence of BESS, the ST-index takes high value. However, this index has low values before the event of outage of wind generator in the presence of BESS. Further, after the high magnitude transients observed after the event of outage of wind generator has been reduced significantly by the use of BESS. This is observed from the Figure 8(c) that at the time of outage of wind generator, values of H-index increase from 640 to 740 indicating that current drawn from the source has increased. However, source current has reduced by small magnitude due to the use of BESS. A small magnitude transient peak observed at the time of event occurrence indicates that disturbances are introduced in the current signal. However, the use of BESS has reduced the disturbances significantly. This can be observed from the Figure 8(d) that at the time of outage of wind generator, the proposed DDI takes high values indicating that significant disturbances are introduced in the current signal. However, the magnitude has been reduced from the value of 350 to 40 by the use of BESS indicating that disturbance level has been reduced significantly (85%) by the use of BESS. However, this index has low values before the event of outage of wind generator. Further, after the event of outage of

wind generator transient components have been reduced significantly in the presence of BESS. This is achieved due to the storage of energy by BESS when high magnitude transient appears and supplying the same energy at the time of dips in the energy levels which helps in the smoothing the output.

4.4. Outage of both wind and solar PV generators

Simultaneous outage of wind and solar PV generators integrated on bus B5 of test system is performed at 0.5 s in the absence of BESS. Current signal is recorded at PCC and depicted in Figure 9(a). Current corresponding to phase-A is decomposed using Stockwell transform and median of absolute values of the output S-matrix is obtained and designated as ST-index which is illustrated in Figure 9(b). This current signal is also decomposed using the Hilbert transform and absolute values of the output is designated as H-index as illustrated in Figure 9(c). Element by element multiplication of proposed ST-index and H-index is obtained and designated as DDI as illustrated in Figure 9(d).

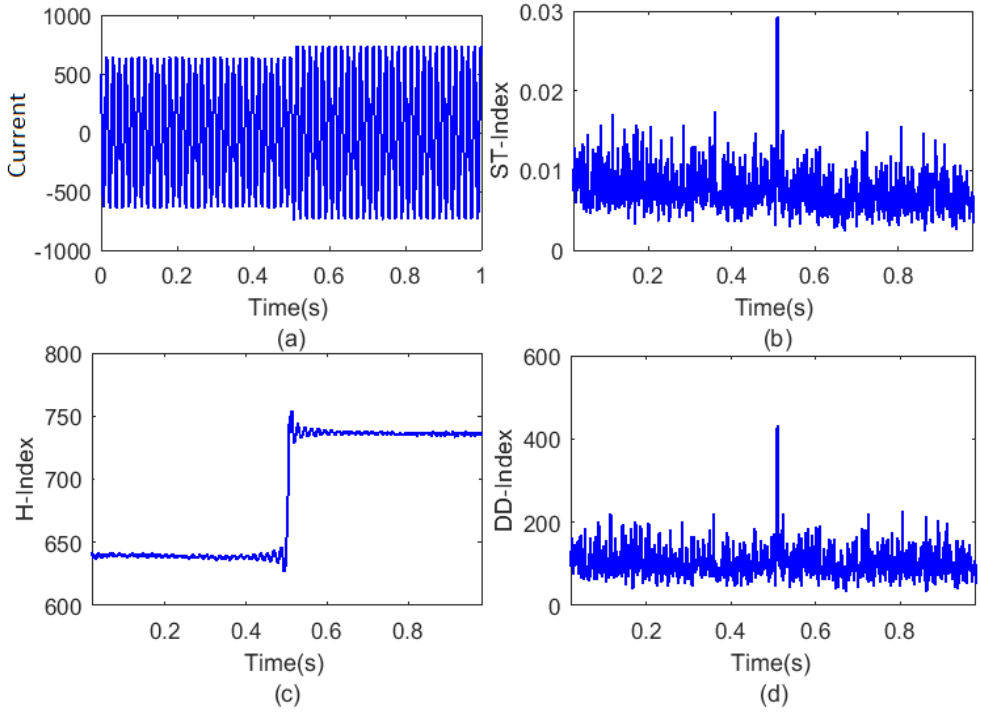

Figure 9. Event of outage of both wind and solar PV generators without BESS (a) current signal (b) ST-index (c) H-index (d) disturbance detection index.

This can be observed from the Figure 9(b) that at the time of simultaneous outage of both wind and solar PV generators in the absence of BESS, the ST-index takes high value. However, this index also has low values before the event of simultaneous outage of both wind and solar PV generators. Further, after the event of outage of generators, transients having significant magnitude are observed. This is observed from the Figure 9(c) that at the time of simultaneous outage of both wind and solar PV generators, values of H-index increase from 640 to 740 indicating that current drawn from the source has increased. A small magnitude transient peak observed at the time of event occurrence

indicates that disturbances are introduced in the current signal. This can be observed from the Figure 9(d) that at the time of simultaneous outage of both wind and solar PV generators, the proposed DDI takes high values indicating that significant disturbances are introduced in the current signal. However, this index has low values of 150 before the event of simultaneous outage of both wind and solar PV generators. Further, after the event of simultaneous outage of both wind and solar PV generators transient components also have values of magnitude equal to 150.

Simultaneous outage of wind and solar PV generators integrated on bus B5 of test system is performed at 0.5 s in the presence of BESS. Current signal is recorded at PCC and depicted in Figure 10(a). Current corresponding to phase-A is decomposed using Stockwell transform and median of absolute values of the output S-matrix is obtained and designated as ST-index which is illustrated in Figure 10(b). This current signal is also decomposed using the Hilbert transform and absolute values of the output is designated as H-index as illustrated in Figure 10(c). Element by element multiplication of proposed ST-index and H-index is obtained and designated as DDI as illustrated in Figure 10(d).

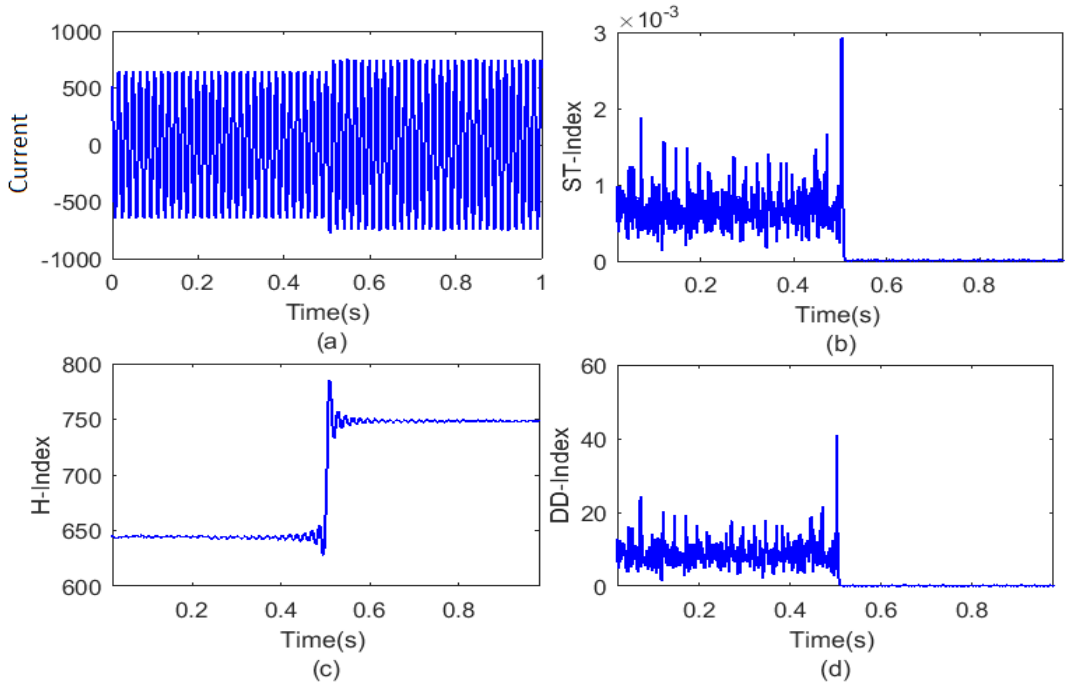

Figure 10. Event of outage of both wind and solar PV generators with BESS (a) current signal (b) ST-index (c) H-index (d) disturbance detection index.

This can be observed from the Figure 10(b) that at the time of simultaneous outage of both wind and solar PV generators in the presence of BESS, the ST-index takes high value. However, this index has very low values before the event of outage of wind generator and these transient have been reduced to zero by the use of BESS. This is observed from the Figure 10(c) that at the time of simultaneous outage of wind and solar PV generator, values of H-index increase from 640 to 740 indicating that current drawn from the source has increased. A small magnitude transient peak observed at the time of event occurrence indicates that disturbances are introduced in the current signal. This can be observed from the Figure 10(d) that at the time of simultaneous outage of wind and solar PV generators, the proposed DDI takes high values indicating that significant disturbances

are introduced in the current signal. However, the peak value of this index has been observed to be 40 by the use of BESS against the 450 observed in the absence of BESS as illustrated in Figure 9(d). Hence, disturbance level is reduced by 91% in the presence of BESS. Further, after the event of simultaneous outage of wind and solar PV generators transient components have been reduced to zero by the use of BESS. This is achieved due to the storage of energy by BESS when high magnitude transient appears and supplying the same energy at the time of dips in the energy levels which helps in the smoothing the output.

5. Conclusions

This research work proposed a battery energy storage system controlled by DSTATCOM for reduction in level of disturbances due to the operational events in hybrid power system. The levels of disturbances are detected in the presence as well as absence of BESS supported by DSTATCOM using an algorithm based on combined features of the Stockwell transform and Hilbert transform. It is concluded that the proposed BESS is effective in reducing the disturbance level in the hybrid power system network due to the operational events such as switching ON/OFF the resistive load, outage of wind generator and simultaneous outage of both wind and solar PV generators. Proposed BESS is found to be effective in reducing the disturbance level maximum up to 91% during the event of simultaneous outage of wind and solar PV generators. Proposed BESS also reduced the oscillatory disturbances completely after the occurrence of evens of switching off the resistive load, switching on the resistive load and simultaneous outage of wind and solar PV generators. Proposed method can be implemented in the utility grid with renewable energy penetration and it will help to increase penetration level of renewable energy by reducing disturbance level.

Conflict of interest

The authors declare no conflict of interests.

References

1. Shaik AG, Mahela OP (2018) Power quality assessment and event detection in hybrid power system. *Electr Pow Syst Res* 161: 26–44.
2. Mahela OP, Shaik AG (2016) Power quality improvement in distribution network using DSTATCOM with battery energy storage system. *Int J Elec Pow* 83: 229–240.
3. Mahmud MA, Pota HR, Hossain MJ (2013) Nonlinear DSTATCOM controller design for distribution network with distributed generation to enhance voltage stability. *Int J Elec Pow* 53: 974–979.
4. Rezvani A, Gandomkar M (2016) Modeling and control of grid connected intelligent hybrid photovoltaic system using new hybrid fuzzy-neural method. *Sol Energy* 127: 1–18.
5. Rezvani A, Gandomkar M (2017) Simulation and control of intelligent photovoltaic system using new hybrid fuzzy-neural method. *Neural Comput Appl* 28: 2501–2518.
6. Dadfar S, Wakil K, Khaksar M, et al. (2019) Enhanced control strategies for a hybrid battery/photovoltaic system using FGS-PID in grid-connected mode. *Int J Hydrogen Energ* 44: 14642–14660.

7. Shi X, Dini A, Shao Z, et al. (2019) Impacts of photovoltaic/wind turbine/microgrid turbine and energy storage system for bidding model in power system. *J Clean Prod* 226: 845–857.
8. Rezvani A, Esmaeily A, Etaati H, et al. (2019) Intelligent hybrid power generation system using new hybrid fuzzy-neural for photovoltaic system and RBFNSM for wind turbine in the grid connected mode. *Front Energ* 13: 131–148.
9. Rikos E, Tselepis S, Hoyer-Klick C, et al. (2008) Stability and power quality issues in microgrids under weather disturbances. *IEEE J-STARS* 1: 170–179.
10. Mahela OP, Shaik AG, Gupta N (2015) A critical review of detection and classification of power quality events. *Renew Sust Energ Rev* 41: 495–505.
11. Dash PK, Padhee M, Panigrahi TK (2012) A hybrid time–frequency approach based fuzzy logic system for power island detection in grid connected distributed generation. *Int J Elec Pow* 42: 453–464.
12. Shao Z, Wakil K, Usak M, et al (2018) Kriging Empirical Mode Decomposition via support vector machine learning technique for autonomous operation diagnosing of CHP in microgrid. *Appl Therm Eng* 145: 58–70.
13. Shi X, Gholamalizadeh E, Moheimani R (2019) Applying a micromechanics approach for predicting thermal conducting properties of carbon nanotube-metal nanocomposites. *J Alloy Compd* 789: 528–536.
14. Mishra M, Sahani M, Rout PK (2017) An islanding detection algorithm for distributed generation based on Hilbert–Huang transform and extreme learning machine. *Sustain Energ Grids* 9: 13–26.
15. Mahela OP, Shaik AG (2015) Power quality detection in distribution system with wind energy penetration using discrete wavelet transform. *2nd International Conference on Advances in Computing and Communication Engineering. IEEE*, 328–333.
16. Sharma A, Ola SR, Mahela OP (2016) Impact of grid disturbances on the output of grid connected wind power generation. *1st International Conference on Power Electronics, Intelligent Control and Energy Systems (ICPEICES). IEEE*, 1–6.
17. Mitra P, Venayagamoorthy GK (2009) An adaptive control strategy for DSTATCOM applications in an electric ship power system. *IEEE T Power Electr* 25: 95–104.
18. Labeeb M, Lathika BS (2011) Design and analysis of DSTATCOM using SRFT and ANN-fuzzy based control for power quality improvement. *IEEE Recent Adv Intell Comput Syst* 274–279.
19. Singh B, Jayaprakash P, Kothari DP (2008) A T-connected transformer and three-leg VSC based DSTATCOM for power quality improvement. *IEEE T Power Electr* 23: 2710–2718.
20. Singh B, Jayaprakash P, Kothari DP (2008) Isolated H-bridge VSC Based 3-phase 4-wire DSTATCOM for power quality improvement. *IEEE Int Conf Sustain Energ Technol IEEE*, 366–371.
21. Singh B, Niwas R, Dube SK (2014) Load leveling and voltage control of permanent magnet synchronous generator-based DG set for standalone supply system. *IEEE T Ind Inform* 10: 2034–2043.

AIMS Press